

## Accurate Measurement of the Cosmic Ray Proton Spectrum from 100TeV to 10PeV with LHAASO

---

**L.Q. Yin<sup>ab</sup>, L.L. Ma<sup>a\*</sup>, Z.Cao<sup>a</sup>, S.S.Zhang<sup>a</sup>, B.Y. Bi<sup>ab</sup> for the LHAASO Collaboration**

<sup>a</sup>Key Laboratory of Particle Astrophysics, Institute of High Energy Physics, CAS, Beijing, China.

<sup>b</sup>University of Chinese Academy of Science, Beijing, China.

E-mail: yinlq@ihep.ac.cn

Large High Altitude Air Shower Observatory (LHAASO) is a composite cosmic ray observatory consisting of three types of detectors: KM2A, WCDA and WFCTA. One of the main scientific objectives of LHAASO is to measure the cosmic ray spectrum and composition precisely. With hybrid detection of WCDA and WFCTA, one can further study the "Knee" of cosmic rays from 100TeV to 10PeV. The original components of cosmic rays can be effectively distinguished with four parameters provided by WFCTA, WCDA and MDA, respectively. The energy reconstruction resolution of proton shower is about 20% reconstructed only by WFCTA. Combining with the energy flow of shower core provided by WCDA, a better energy resolution is expected.

*35th International Cosmic Ray Conference — ICRC2017  
10–20 July, 2017  
Bexco, Busan, Korea*

---

\*Speaker.

## 1. Introduction

The origin and acceleration of cosmic rays have been a puzzle for more than 100 years. In 2002, the origin of cosmic rays was as one of the eleven major frontier scientific problems in the new century [1]. The basic knowledge about energy spectrum of cosmic rays has been obtained by both space and ground observation. Energy spectrum of cosmic rays follows a simple power law, of which power exponent  $\gamma$  is about -2.7, over a very broad energy range from  $10^9$  eV to  $10^{20}$  eV; And there are four fine structures: the knee around  $3 \times 10^{15}$  eV where the spectral index  $\gamma$  changes from -2.7 to -3.1, second knee around  $4 \times 10^{17}$  eV where  $\gamma$  changes from -3.1 to -3.3, ankle about  $4 \times 10^{18}$  where  $\gamma$  changes from -3.3 to -2.7 again, and probable GZK cutoff [2] around  $6 \times 10^{19}$ .

The cause of these four fine structures is closely related to the origin and acceleration mechanism of cosmic rays. It is generally believed that: extragalactic cosmic rays begin to occupy the dominant position from the knee region. There are several models that explain the causes of knee, such as galactic shock waves acceleration upper limit [3], leaky box model [4] and threshold effect [5]. The first model is widely accepted: the extension of the acceleration region and the strength of the magnetic field limit the highest energy of galactic cosmic rays that can be accelerated.

Due to the limitation of space payload, the low cosmic ray flux and large statistical error at high energy, it is difficult for space experiments to detect the cosmic rays above 100 TeV. Therefore, cosmic rays above 100 TeV have to be measured by ground based experiments. These experiments detect the extensive air showers (EAS) produced by the interactions of cosmic particles with nuclei of the atmosphere. However, it is difficult to determine the energy and mass of primary particles because of the large intrinsic fluctuations of EAS. Thus, the lack of absolute energy calibration of the detectors and relative energy calibration between different experiments caused a chaotic situation in measurement of energy spectrum of individual component at knee region [6].

One of the main science object of Large High Altitude Air Shower Observation (LHAASO) [7] [8] is to precisely measure the cosmic rays energy spectrum of individual components from  $10^{14}$  eV to  $10^{18}$  eV. It means to solve the chaotic situation in measurement of energy spectrum through hybrid detection by four sub-detectors: electromagnetic detector (KM2A-ED), Muon detector (KM2A-MD), water cherenkov detector array (WCDA) and wide field of view cherenkov telescope array (WFCTA).

In section 2, the description for detectors is presented; In section 3, data used for this simulation is introduced; and the reconstruction resolution of shower geometry and energy are presented. In section 4, the four component sensitive variables are discussed; and the selection of a high purity sample of  $P + He$  is described. Section 5 shows the energy spectrum and statistics of a year at different models. Section 6 gives the conclusion.

## 2. Detectors and Measurements

LHAASO is located in Daocheng Haizishan, 4300m a.s.l., Sichuan Province, Chian. It is a perfect altitude to study the knee physics. LHAASO was formally approved in December 31, 2015 and now is under construction. One quarter array of LHAASO is planned to be completed in 2018 and the full array will be completely operated by 2021.

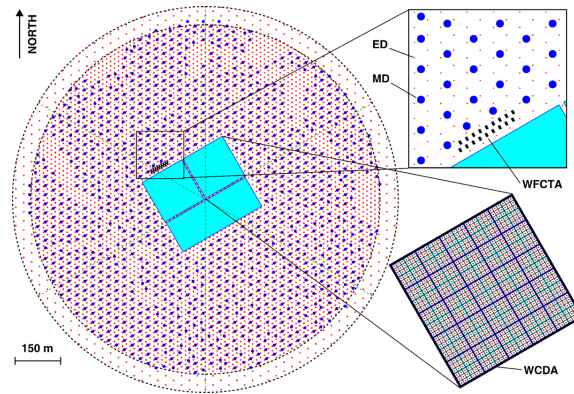


**Figure 1:** The detectors layout of LHAASO experiment.

WFCTA is one of the main detector arrays of LHAASO. Each telescope has a spherical mirror of which the effective area is  $5m^2$  to collect Cherenkov light. The camera is consist of 1024 SiPM and the pixel of each SiPM is  $0.5^\circ$ , watching a FOV of  $14^\circ \times 16^\circ$ . The camera is followed by electronic system. All the parts of telescope are placed in a container for the convenience of movement and arrangement. Additionally, two telescopes prototype have been operated successfully at YBJ cosmic ray observatory in Tibet [9]. The WFCT works like IACT. It can watches EAS longitudinal development. Total number of photoelectrons in the Cherenkov image is a great EAS energy estimator. And shape of Cherenkov image is sensitive to primary particles, such as the ratio of length (L) and width (W) of cherenkov image.

WCDA is a water Cherenkov detector array with a total area of  $78,000 m^2$  [10]. It consists of three water pond, two have a  $150m \times 150m$  and one has a  $300m \times 110m$ , with a depth of 4.5 m. Each pond is divided into small cells of  $5m \times 5m$ , and an 8 inch Photomultiplier Tubes (PMT) anchored on the bottom at the center of the cell. At one of  $150m \times 150m$  ponds, a 1 inch PMT is also placed in each cell; and the dynamic range is from 50 to 500,000 photons. This pond is called WCDA++, of which primary objective is to achieve the hybrid detection with the WFCTA. WCDA detects the Cherenkov light produced in water by cascade processes of secondary electrons and photons in EAS that falling into the cell. Therefore the energy flow measured by WCDA is also a good energy estimator.

The square kilometer array (KM2A) is the main array of LHAASO. KM2A contains two sub-array: electromagnetic detector array (EDA) and Muon detector array (MDA). In this simulation, only MDA is included. MDA is an array of underground water Cherenkov detectors [11]. The area of each muon detector is  $36 m^2$  and there are 1213 muon detectors covering the  $1 km^2$  area with a spacing of 30m. As shown in FIG. 1 as the blue dots. With the largest muon detector array, it can be well measured that the number and lateral distribution of muon which is a powerful parameter to identify the primary particle.

The hybrid experiment of ARGO-YBJ and two WFCTs prototypes has given important results [12]: the energy spectrum of proton+helium has a knee at  $E_k = 700 \pm 230(stat) \pm 70(sys)$  TeV, where the spectral index changes from  $-2.56 \pm 0.05$  to  $-3.24 \pm 0.36$ . It made a preliminary study for LHAASO hybrid detection. WCDA is similar to ARGO-YBJ detector as the "carpet" detector array; and WFCTs will have smaller pixels  $0.5^\circ$  than the two prototypes  $1^\circ$  with the same FOV.

Hence, based on the analysis in hybrid detection of ARGO-WFCTs, the simulation for LHAASO hybrid observation is carried out.

### 3. Simulations and Reconstructions

The simulated data is generated by CORSIKA program. The program version is 6990 and EGS4 model is chosen for electromagnetic interaction; the QGSJET02 and GHEISHA models are chosen for high and low energy hadronic process respectively. Both Cherenkov data and particles data are recorded to do the hybrid observation. Five components, proton, helium, CNO, MgAlSi and iron with energy from 100TeV to 10PeV are generated according to a power law spectrum with a index of -2.7. The directions of the showers are from 24° to 38° in zenith and from 77° to 103° in azimuth. This data is generated for simulation of the hybrid observation of two prototypes of WFCT and ARGO-YBJ. New data for LHAASO simulation and the related analytical work is under way.

The simulation of LHAASO detectors are performed separately. The simulated results of different detectors are integrated with the events number. The shower geometry reconstruction, the core positions and the arriving directions, can be obtained by WCDA through NKG fitting method. For proton, the shower core position resolution is less than 3m and the arrival direction resolution is 0.3°. As shown in FIG. 2 (left).

The energy reconstruction is obtained by WFCTA. There is a linear correlation between shower energy  $E$  and the corrected number of Cherenkov photoelectrons,  $N_0^{pe}$ .  $N_0^{pe} = \log_{10} N^{pe} + a \times (R_p/1m) + b \times \tan \alpha$ , where  $N^{pe}$  is total number of photoelectrons collected by WFCT directly;  $R_p$  is the distance from telescope to the shower axis; and  $\alpha$  is the space angle between the shower direction and the optical axis of the telescope. The parameters  $a$  and  $b$  can be a little different for different mass ingredients of particles.

For proton,  $a = 0.0083$  and  $b = 0.0142$ ; the reconstructed energy is  $E_{rec} = 10^{0.95 \times N_0^{pe} - 2.2}$ . The reconstructed bias and resolution are shown in FIG. 2 (right). Moreover, particle identification is performed before energy reconstruction when dealing with observed data.

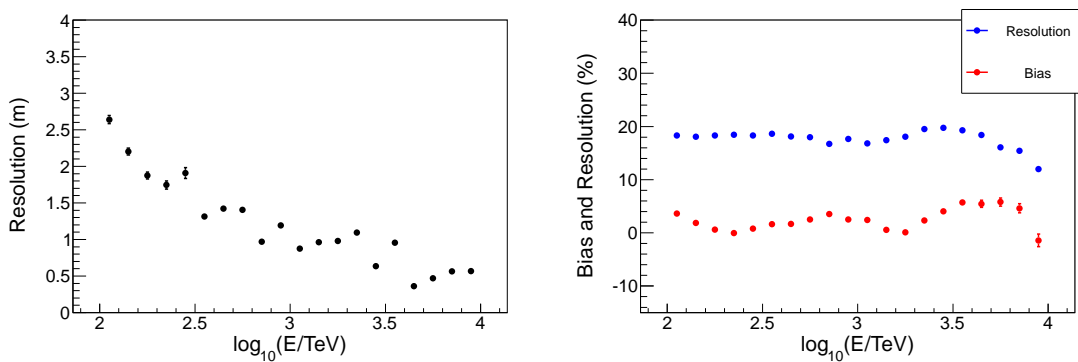


**Figure 2:** The reconstruction of proton above 100TeV; the left plot shows the resolution of shower core position; and the right plot shows the reconstructed resolution and bias of shower energy.

#### 4. Identification of primary particles

In this hybrid observation, four independent variables,  $P_F$ ,  $P_C$ ,  $P_X$ ,  $P_\mu$ , can be used for particles distinguish.

$P_F$  is energy flow near the core provided by WCDA. This variable is constructed by the total number of equivalent photoelectrons  $W_{max}$  recorded by the small PMT in the fired cell. The formula is expressed as  $P_F = \log_{10}W_{max} - 1.182\log_{10}N_0^{pe}$ .

$P_C$  is constructed by the ratio of length and width (L/W) of a Cherenkov image measured by WFCTA. Expression as  $P_C = L/W - 0.0137R_p + 0.239\log_{10}N_0^{pe}$ .

The angular distance  $\Delta\theta$  between centroid of the Cherenkov image and the shower direction could be used to measure the atmospheric depth for shower maximum  $X_{max}$  which is sensitive to particles. Since showers initiated by heavy primaries start earlier in the atmosphere, the  $X_{max}$  is smaller than that of light primaries. The variable  $P_X$  is constructed by  $\Delta\theta$  expressed as  $P_X = \Delta\theta - 0.0103R_p - 0.404\log_{10}N_0^{pe}$ .

The muon lateral distribution measured by muon detector array can be fitted by the formula(4.1) which is similar to the NKG function.

$$\rho(r, N_\mu) = k_G N_\mu \left(\frac{r}{r_G}\right)^{-a} \left(1 + \frac{r}{r_G}\right)^{-b} [m^{-2}] \quad (4.1)$$

where  $a \cong 1.4$ ,  $b \cong 1.0$ ,  $r_G \cong 220m$ . The total number of muon  $N_{mu}$  heavily depend on the primary mass. The higher nucleon number, the larger muon content at observation level. Hence the variable  $P_\mu = \log_{10}N_\mu - 0.929\log_{10}N_0^{pe}$  is powerful for particle identification.

The distribution of  $P_F$  and  $P_\mu$  for different mass group is shown in FIG. 3.

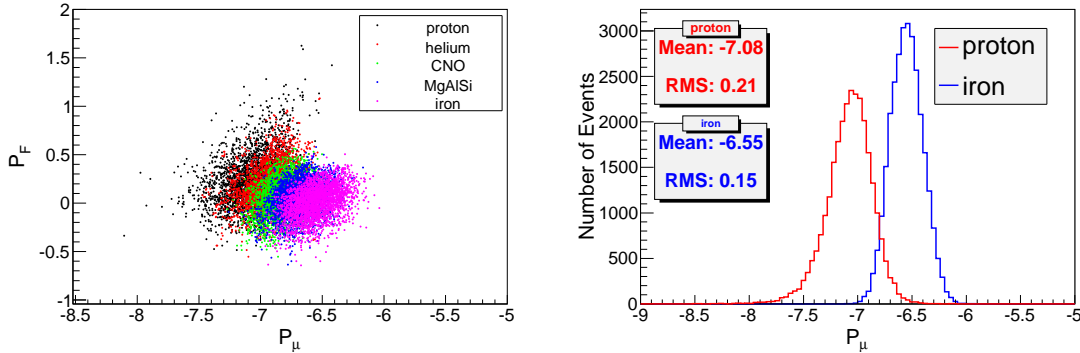


**Figure 3:** The correlation between the parameters  $P_F$ ,  $P_\mu$  for different species of mass group (left plot). The  $P_\mu$  distribution for proton and iron is shown in the right plot.

The method of Multi Variable Analysis (MVA) to identify the primary particles is described in another paper. Here, a simple event-by-event cut by using of  $P_F$  and  $P_\mu$  could also do a good job to distinguish the primaries. The FIG. 4 shows the aperture and contamination of particle group  $P + He$  for an identification example. The aperture of proton and proton+helium are around  $1500 m^2 Sr$  and  $4000 m^2 Sr$  respectively by this method; and the purity of proton can reach 90% and purity of proton+helium is more than 95%.

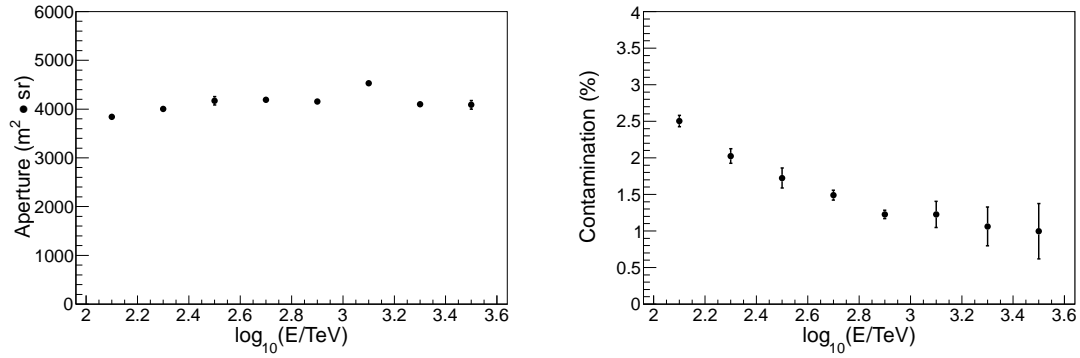


**Figure 4:** The aperture (left) and contamination (right) of particle group  $P + He$  through event-by-event cut by using  $P_F$  and  $P_\mu$ .

## 5. Spectrum expectation and event rate

The statistics of one year has been estimated with the full LHAASO array under different models; and the statistical errors are also evaluated under these models respectively. This expectation is based on the event selection mentioned above.

Three models are used: the spectrum measured at the hybrid detection of ARGO-YBJ and prototype of WFCTs, the Horandel model and the H4A model. The duty cycle of hybrid observation is set as 10% mainly depending on the cherenkov telescope.

There are more than 2500 pure proton events above 700TeV with the model of ARGO-WFCTA, and the statistics of proton+helium is doubled as shown in FIG. 5. Since the iron analysis of ARGO-WFCTA experiment is not carried out, no results for iron.

About 3000 pure proton events above 700TeV with the Horandel model; the statistics of proton+helium is around 20000 as shown in FIG. 6.

With the H4A model, about 4000, 30000 events can be sampled for proton and proton+helium respectively above 700TeV as shown in FIG. 7.

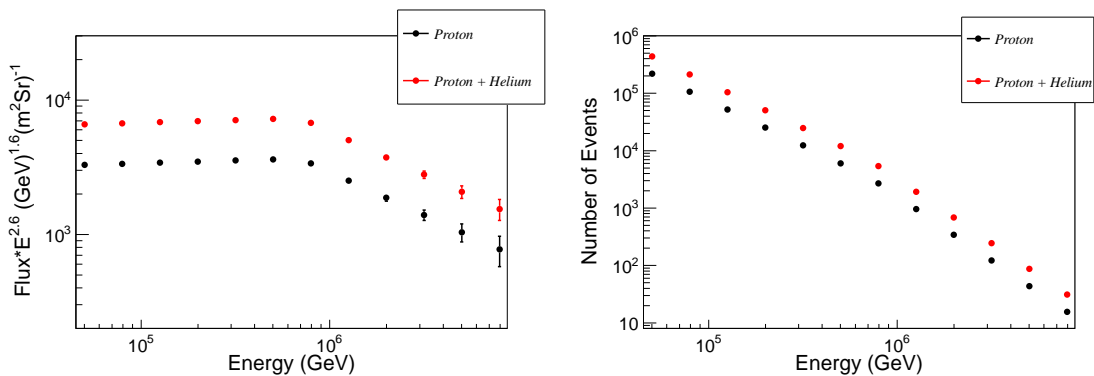


**Figure 5:** Energy Spectrum (left) of individual components or mass groups at ARGO-WFCTA model and the corresponding statistics (right) of a year.

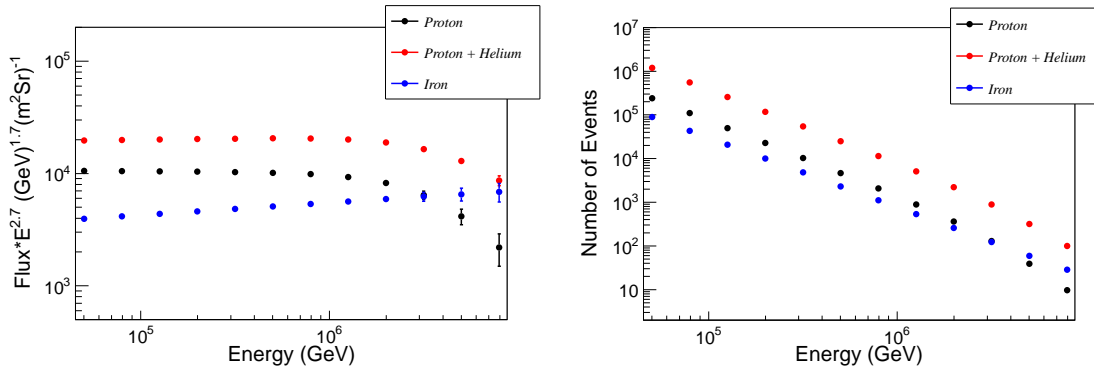


**Figure 6:** Energy Spectrum (left) of individual components or mass groups at Horandel model and the corresponding statistics (right) of a year.

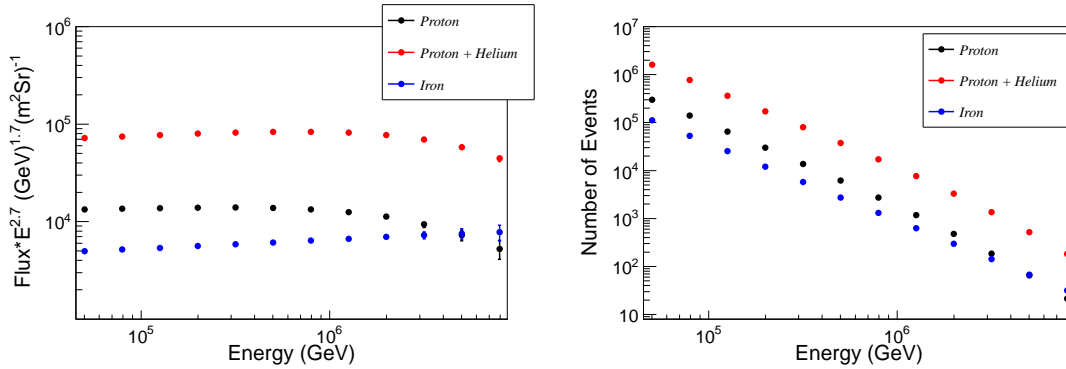


**Figure 7:** Energy Spectrum (left) of individual components or mass groups at H4A model and the corresponding statistics (right) of a year.

## 6. Summary and Propection

The present study of hybrid detection with WFCTA, WCDA and MDA following the method of ARGO-WFCTA [12] provides promising prospect. Moreover, WCDA can measure the remaining shower energy which is relatively complemented with the energy deposition in the air measured by WFCTA. This study about the uses of energy flow for energy reconstruction is in process. So in LHAASO hybrid measurement, we hope a improvement of the energy resolution and reduction of the systematic dependence of the primary composition.

## 7. Acknowledgements

This work is supported by National Natural Science Foundation (NSFC) of China under contacts No. 11635011.

## References

- [1] E.Haseltine, The greatest unanswered question of physics, Discover(2002).

- [2] K. Greisen, Phys. Rev. Lett., 1966, 16.
- [3] P. Lagage, C. Cesarsky, Astronom. Astrophys., 1983, 125: 249-257.
- [4] M. M. Shapiro, et al., Annu. Rev. Nucl. Sci., 1970, 20(20): 323-392.
- [5] A.A. Petrukhin., Physics of Atomic Nuclei, 2003, 66(3): 517-522.
- [6] V. Berezhinsky, J. Phys. Conf. Ser., 2008, 120(1): 012001.
- [7] Z. Cao (for LHAASO Coll.), Chin.Phys. C34 (2010) 249-252.
- [8] Z. Cao (for LHAASO Coll.), 31th ICRC, LORZ,(2009).
- [9] S.S.Zhang et al., Nucl.Instrum.Meth. A, 2012, 629(1)57-65.
- [10] Q. An et al (for LHAASO Coll.), Nucl.Instrum.Meth. A, 2013, 724: 12-19.
- [11] X. Zuo et al (for LHAASO Coll.), Nucl.Instrum.Meth. A, 2015, 789: 143.
- [12] B. Bartoli et al (ARGO-YBJ and LHAASO Coll.), Phys. Rev. D, 2015, 92(9): 25-31.